

Comparison of Bridge Pier Scour by Using Numerical Simulations with FLUENT and Field Observation

¹May Than Zaw, ²Cho Cho Thin Kyi, ³Win Win Zin

^{1,2,3}Department of Civil Engineering, Yangon Technological University,
Yangon, Myanmar

Email – ¹maythanzaw@gmail.com, ²ccthinkyi@gmail.com, ³winwinzin@gmail.com

Abstract: In this paper, the scour depth around the pier is compared between the numerical simulations and field observation results. The study area, Maubin Bridge, is situated on the Yangon- Sarmalout- Maubin highway crossing upon Toe River, Maubin Township. Firstly, the scour depths are observed by using field observation data. Using the Fluent and Gambit software, scour depths are estimated by simulating to flow field around bridge piers and scour patterns around the piers are developed. Finally, it is observed that a satisfactory agreement is achieved between the results of numerical simulation and the observation.

Key Words: Scour depth, bridge pier, numerical simulation, field observation, scour pattern.

1. INTRODUCTION:

Scour is the removal of sediment around or near structures located in flowing water. Scour also occurs at the coastal regions as a result of the passage of waves. It is the removal of sediment around or near structures located in flowing water. The most common cause of bridge failures is from floods scouring bed material from around bridge foundations. Scour is the engineering term for the erosion caused by water of the soil surrounding a bridge foundation (piers and abutments). Flowing water can excavate and carry away materials from the river bed and from around the piers and abutments of bridges, thus resulting in scour hole. Formation of scour may weaken bridge foundation and in extreme cases bridge failures occur. The construction of bridges in alluvial channels causes a contraction in the waterway at the bridge site and hence gives rise to significant scour at that site.

There are generally three types of scours that affect the performance and safety of bridges, namely, local scour, contraction scour and degradation scour. Local scour is the removal of sediment from around bridge piers or abutments. When water is flowing through the piers or abutments, it may evacuate sediment around the pier and creates scour holes. This removal of sediment is caused mainly due to the formation of both horse vortex and down flow in front of the piers. Wake vortices are formed as the flow, which is separated by the pier, converges at the downstream of the pier. With the increase in scour depth, the horseshoe vortex strength reduces, which automatically leads to a reduction in the sediment transport rate from the base of the pier.

Improving the understanding of the local scour phenomena is therefore vital to the engineer responsible for the design of pier foundations. The knowledge of the maximum possible scour around a bridge pier is of paramount importance in safe and economic design of foundations of bridge piers. Prediction of local scour holes plays an important role in bridge foundation design. Underestimation of the scour depth results in too shallow design of a foundation, which may consequently become exposed to the flow endangering the safety of the bridge. Overestimation of the scour depth results in too deep design of a foundation, which is not economical design. Excessive local scour can progressively undermine the foundation of the structure. Because complete protection against scour is too expensive, generally, the maximum scour has to be predicted to minimize the risk of failure.

FLUENT is the world leading CFD code for a wide range of flow modeling applications. With its long-standing reputation of being user-friendly, FLUENT makes it easy for new users to come up to productive speed. Its unique capabilities in an unstructured, finite volume based solver are near ideal in parallel performance. GAMBIT is used as a tool to generate or import geometry so that it can be used as a basis for simulations run in FLUENT.

The aim of the study is to evaluate existing bridges for scour vulnerability, to verify computational fluid dynamics model for local scour around cylindrical pier and to apply the computer software package, FLUENT, to simulate the complex flow field and local scour.

2. CHARACTERISTICS OF STUDY AREA:

The study area, Maubin Bridge, is situated on the Yangon- Sarmalout- Maubin highway crossing upon Toe River, Maubin Township, Ayeyarwaddy Region. It was opened on 10 February 1998, to commemorate the 51st Anniversary Union Day. The Maubin Bridge was built across the Ayeyarwaddy River's tributary named the Toe River to link the Twantay-Maubin road and the Maubin-Hsarmalauk road with the Maubin-Yaylegalay-Shwetaunghmaw Mawlamyinegyun road and Maubin-Kyaiklat road. The bridge is located near Talok East and Talok West villages in Maubin Township, Ayeyarwaddy Division. The bridge is 721.8 metres long. The bridge has two approach bases and

three mid-river piers. Maubin Bridge was being built to improve transportation and in order to narrow down the development gap. Before its existence, Z crafts were used to reach Maubin across the Ayeyarwaddy River. There was great delay congestion and inefficiency at this critical point. After the completion of the bridge, there is no more such grave situation and it shortens the traveling time in an incredible scale. So it is very important to maintain the bridge and guarantee the safety of the bridge.

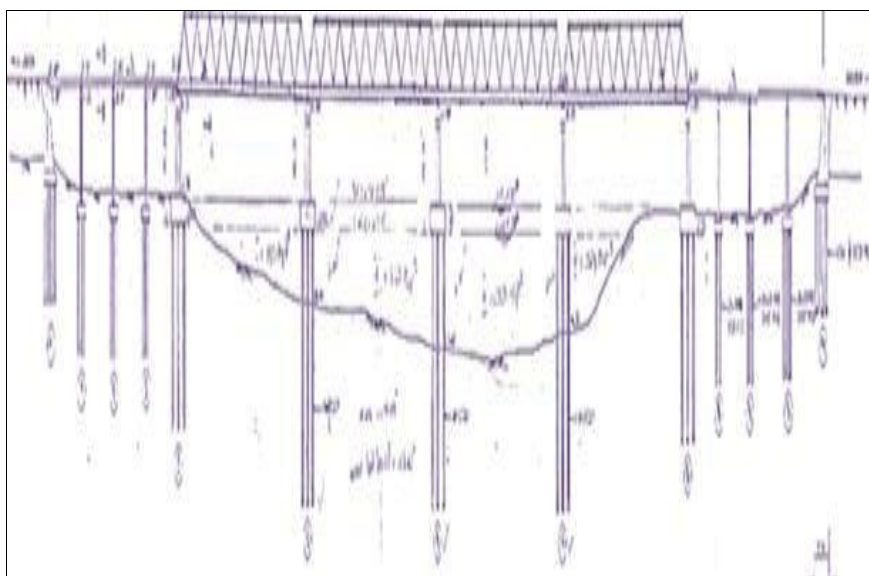


Fig 1(a). General View of Maubin Bridge



Fig.1 (b). Study Area Map

3. METHODOLOGY:

This study investigates CFD (Computation Fluid Dynamics) Eulerian two-phase model compared with field data.

CFD Numerical Simulation

Computational Fluid Dynamic (CFD) is the analysis of systems by means of computer-based simulation. The advent of high-speed and large memory computers has enabled CFD to solve many flow problems (including those are compressible or incompressible, laminar or turbulent, chemically reacting and multiphase) in a reasonable time. Computational Fluid Dynamic (CFD) codes cover the numerical solution of the Navier-Stokes equations in three dimensional and offer several properties for their extension. The methods of discretization in CFD are Finite Difference Method (FDM), Finite Volume Method (FVM), Finite Element Method (FEM), and the Boundary Element Method (BEM).

There are many advantages to use CFD including low cost, quick solutions, scale up, comprehensive solutions and safe options. The standard equations of continuity, momentum, and energy conservation are solved on a non-staggered grid by a finite volume approach. The $k-\epsilon$ model provides closure for turbulence. One advantage of this solver is continuity and momentum equation.

Governing Equations

The continuity and the momentum equations are as given below:

Continuity equation

$$\left(\frac{\partial u}{\partial x} + \frac{\partial u}{\partial y} + \frac{\partial u}{\partial z}\right) = 0 \quad (1)$$

Momentum equations

x-direction:

$$\rho \left(\frac{\partial u}{\partial t} + u \frac{\partial u}{\partial x} + v \frac{\partial u}{\partial y} + w \frac{\partial u}{\partial z}\right) = -\frac{\partial p}{\partial x} + \rho g_x + \mu \left(\frac{\partial^2 u}{\partial x^2} + \frac{\partial^2 u}{\partial y^2} + \frac{\partial^2 u}{\partial z^2}\right) \quad (2)$$

y-direction:

$$\rho \left(\frac{\partial v}{\partial t} + u \frac{\partial v}{\partial x} + v \frac{\partial v}{\partial y} + w \frac{\partial v}{\partial z}\right) = -\frac{\partial p}{\partial y} + \rho g_y + \mu \left(\frac{\partial^2 v}{\partial x^2} + \frac{\partial^2 v}{\partial y^2} + \frac{\partial^2 v}{\partial z^2}\right) \quad (3)$$

z-direction:

$$\rho \left(\frac{\partial w}{\partial t} + u \frac{\partial w}{\partial x} + v \frac{\partial w}{\partial y} + w \frac{\partial w}{\partial z}\right) = -\frac{\partial p}{\partial z} + \rho g_z + \mu \left(\frac{\partial^2 w}{\partial x^2} + \frac{\partial^2 w}{\partial y^2} + \frac{\partial^2 w}{\partial z^2}\right) \quad (4)$$

u, v, w	=	velocity component of x, y, z directions
ρ	=	density of material
p	=	pressure
g	=	acceleration of gravity (9.81 m/s ²), (32.2 ft/s ²)
μ	=	dynamic viscosity
t	=	flow time

Governing Equations of Modeling Multiphase Flows

Eulerian Model

The Eulerian model is the most complex of the multiphase models in FLUENT. It solves a set of momentum and continuity equations for each phase. Coupling is achieved through the pressure and inter-phase exchange coefficients. The manner in which this coupling is handled depends upon the type of phases involved; granular (fluid-solid) flows are handled differently than non-granular (fluid-fluid) flows. For granular flows, the properties are obtained from application of kinetic theory. Momentum exchange between the phases is also dependent upon the type of mixture being modeled.

Volume Fractions

The description of multiphase flow as interpenetrating continua incorporates the concept of phase volume fractions, denoted here by α_q . Volume fractions represent the space occupied by each phase, and the laws of conservation of mass and momentum are satisfied by each phase individually. The volume of phase q, V_q , is defined by

Conservation Equations

The continuity equation for phase q is

$$\frac{\partial}{\partial t} (\alpha_q \rho_q) + \nabla (\alpha_q \rho_q V_q) = \sum_{p=1}^m m_{pq} \quad (5)$$

where, V_q is the velocity of phase q and m_{pq} characterizes the mass transfer from the pth to qth phase.

Conservation of Momentum

The momentum balance for phase q yields

$$\frac{\partial}{\partial t} (\alpha_q \rho_q V_q) + \nabla (\alpha_q \rho_q V_q V_q) = -\alpha_q \nabla p + \nabla \tau_q + \sum_{p=1}^n (R_{pq} + m_{pq} V_{pq}) + \alpha_q \rho_q (F_q + F_{lift,q} + F_{vm,q}) \quad (6)$$

where, q is the qth phase stress-strain tensor.

Turbulence Models

The laws of mass, momentum and energy conservation govern Laminar and turbulent flows. Modeling of turbulent flows requires appropriate modeling procedures to describe the effects of turbulent fluctuations velocity and

scalar quantities on the basic conservation equations for laminar flow. FLUENT uses the standard Reynolds' averaging of the conservation and momentum equations.

In comparison to single-phase flows, the number of terms to be modeled in the momentum equations in multiphase flows is large, and this makes the modeling of turbulence in multiphase simulations extremely complex. FLUENT provides mixture turbulence model in multiphase flows within the context of the $k-\epsilon$ models.

The mixture turbulence model is default multiphase turbulence model. It represents the first extension of the single-phase $k-\epsilon$ model, and it is applicable when phases separate, for stratified (or nearly stratified) multiphase flows, and when the density ratio between phases is close to one. In these cases, using mixture properties and mixture velocities is sufficient to capture important features of the turbulent flow.

k-ε models

Two-equation $k-\epsilon$ models, turbulent kinetic energy k and turbulent dissipation ϵ , are the simplest and the most widely used models among all turbulence models that aim to study the effect of turbulence in the flow. Two-equation model signifies that it includes two extra transport equations to represent turbulence properties of the flow. There are three different models that are derived from $k-\epsilon$ model standard $k-\epsilon$ model, Realizable $k-\epsilon$ model and Renormalization Group model (RNG). Despite of having the two general equations, these turbulence models use the different ways to calculate the principle form of the eddy viscosity equation

The turbulence kinetic energy k and its rate of dissipation, ϵ are obtained from the following transport equations

$$\frac{\partial}{\partial t}(\rho k) + \frac{\partial}{\partial x_i}(\rho k u_i) = \frac{\partial}{\partial x_j} \left[\left(\mu + \frac{\mu_t}{\sigma_k} \right) \frac{\partial k}{\partial x_j} \right] + G_k + G_b - \rho \epsilon - Y_M + S_k \quad (7)$$

$$\frac{\partial}{\partial t}(\rho \epsilon) + \frac{\partial}{\partial x_i}(\rho \epsilon u_i) = \frac{\partial}{\partial x_j} \left[\left(\mu + \frac{\mu_t}{\sigma_\epsilon} \right) \frac{\partial \epsilon}{\partial x_j} \right] + C_{1\epsilon} \frac{\epsilon}{k} (G_k + C_{3\epsilon} G_b) - C_{2\epsilon} \frac{\epsilon^2}{k} + S_\epsilon \quad (8)$$

G_k = the generation of turbulence kinetic energy due to the mean velocity gradient

G_b = the generation of turbulence kinetic energy due to buoyancy

Y_M = the contribution of the fluctuating dilatation in compressible turbulence to the overall dissipation rate

$C_{1\epsilon} = 1.44, C_{2\epsilon} = 1.92, C_{\mu} = 0.09, \sigma_k = 1.0, \sigma_\epsilon = 1.3$. These values are user-modifiable constant.

Physical Models in ANSYS Fluent

ANSYS Fluent provides comprehensive modeling capabilities for a wide range of incompressible and compressible, laminar and turbulent fluid flow problems. Steady-state or transient analyses can be performed. In ANSYS Fluent, a broad range of mathematical models for transport phenomena (like heat transfer and chemical reactions) is combined with the ability to model complex geometries.

Another very useful group of models in ANSYS Fluent is the set of free surface and multiphase flow models. These can be used for analysis of gas-liquid, gas-solid, liquid-solid, and gas-liquid-solid flows. For these types of problems, ANSYS Fluent provides the volume-of-fluid (VOF), mixture, and Eulerian models, as well as the discrete phase model (DPM).

For all flows, ANSYS Fluent solves conservation equations for mass and momentum. For flows involving heat transfer or compressibility, an additional equation for energy conservation is solved. For flows involving species mixing or reactions, a species conservation equation is solved or, if the non-premixed combustion model is used, conservation equations for the mixture fraction and its variance are solved. Additional transport equations are also solved when the flow is turbulent.

Empirical Scour Equations for Local Scour

There are many predictive empirical equations for local scour depth in the literature. These equations differ significantly in their form and in the magnitude of their predictions. The recommended equation developed at Colorado State University in its Hydraulic Engineering Circular No.18 Report, HEC-18

$$d_{se} = 2.0 K_1 K_2 K_3 K_4 b^{0.65} y^{0.35} Fr^{0.43} \quad (9)$$

where,

d_{se} = equilibrium scour depth,

y = flow depth upstream of structure,

K_1 = correction factor for pier nose shape,

K_2 = correction factor for angle of attack flow,

- K_3 = correction factor for bed condition,
- K_4 = correction factor for armoring by bed material size,
- b = pier width,
- $Fr = V_0/(gy_0)^{1/2}$, Froude Number,
- V_0 = Mean velocity of flow directly upstream of the pier
- g = acceleration of gravity ($9.8m/s^2$) ($32.2 ft/s^2$)

4. FIELD OBSERVATION:

Observed Bed Level Data

The observed bed level data are taken from the Directorate of Water Resources and Improvement of River System (DWIR).

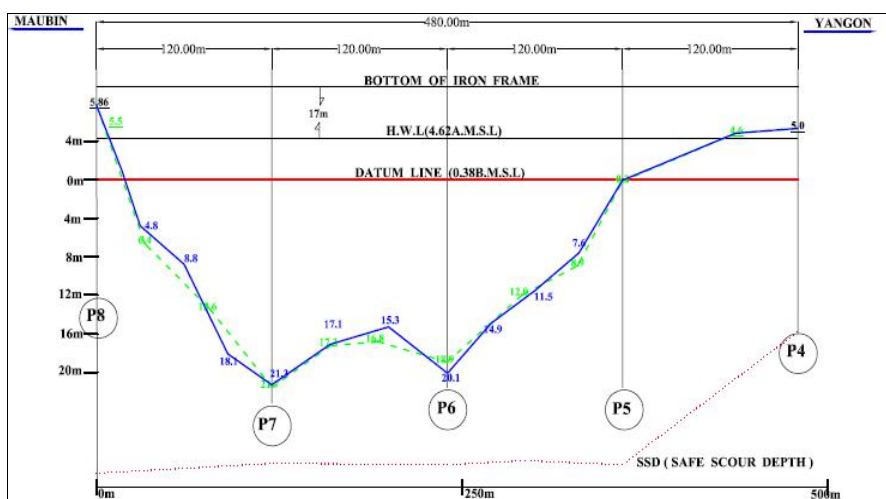


Fig.2 Cross sectional profile of design foundation of Maubin Bridge

Scour around Piers of Maubin Bridge

Scour around piers, P-4 to P-8 are shown in Table. Since the construction of the bridge was completed and the bridge was opened, the existing problem of erosion at Maubin bank was enhanced and accelerated, and became a threat to the bridge. Bank erosion problems was found to be the main cause in Maubin Bridge. In order to solve the problems, a lot of river training structures and bank protection works have been implemented.

TABLE I
 SCOUR DEPTH AROUND A BRIDGE PIER

Date	P8	P7	P6	P5	P4
2010	5.86	-17	-18	-4.9	5.3
2011	5.86	-19.3	-16.1	-5.2	5.3
2012	5.86	-20	-17	-5.7	5.3
2014	5.86	-20.6	-19	-5.0	5.3
2015	5.86	-17.4	-17.9	-1.2	5.3
2016	5.86	-21.7	-18.9	-0.2	5.3
2017	5.86	-21.3	-20.1	-0.1	5.3

Bed level changes

The bed level changes are shown in Figure 3. The bed level from high water period in 2010, 2011, 2012, 2014, 2015, 2016 and 2017 have the changes at P7, P6 and P5. There are adequacy and inadequacy of bank protection works which are visible in reviewing the bed level changes from 2010 to 2017.

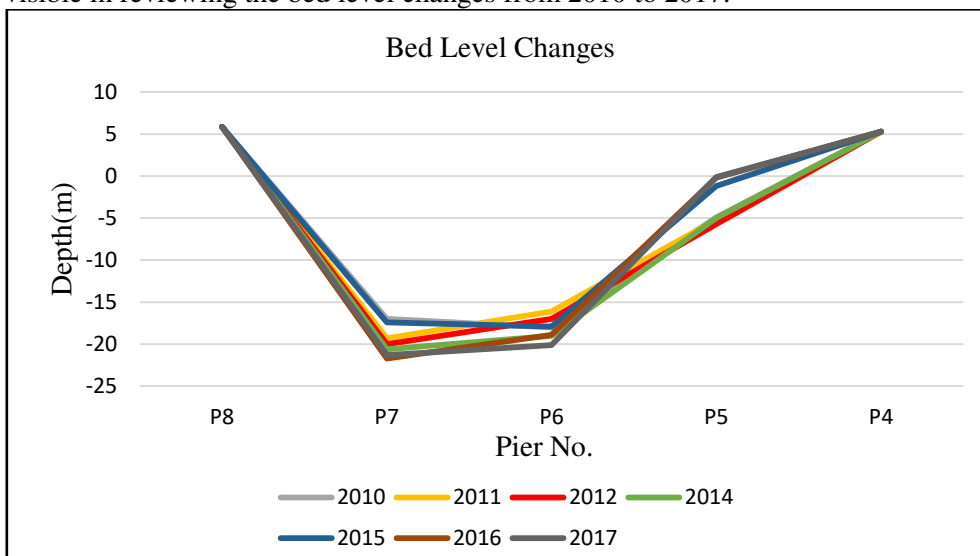


Fig.3 Bed level changes

5. NUMERICAL METHOD:

Gambit and Mesh Generation

FLUENT is a two part program consisting of a pre-processor, GAMBIT, and a main module, FLUENT. GAMBIT was used to define the geometry and a structured grid of the problem to be modeled. The grid information was then imported from GAMBIT to FLUENT.

Geometric Setup

In the finite difference solution, the absolute size of cells within the grid is an important issue, since if the cells are too large, the solution obtained can be dependent on the cell size rather than purely on the physical constraints of the solution domain and the input conditions. For the present simulation, a three-dimensional grid system was generated by GAMBIT for the FLUENT simulation.

After several trial runs, the present grid arrangement was found satisfactory. The geometry of the flow zone for numerical simulation is generated by GAMBIT. The whole zone of the flow field is cuboids. The numbers of mesh are considered in 3 dimensions of length, width and height are 482x482x30 for model. A cylinder is placed at 241m from the center of the cuboids and its diameter is 1.8m for model. The grids of the simulation generated by GAMBIT are shown in Fig.4.

The grid close to the pier has much higher density than those away from it. Grid spacing increases gradually in the radial direction from the pier center. The grids near the cylinder are generated more densely because the flow in the region is more complex. The grid spacing use an interval size of 3 (the default).The mesh volume is 294500.

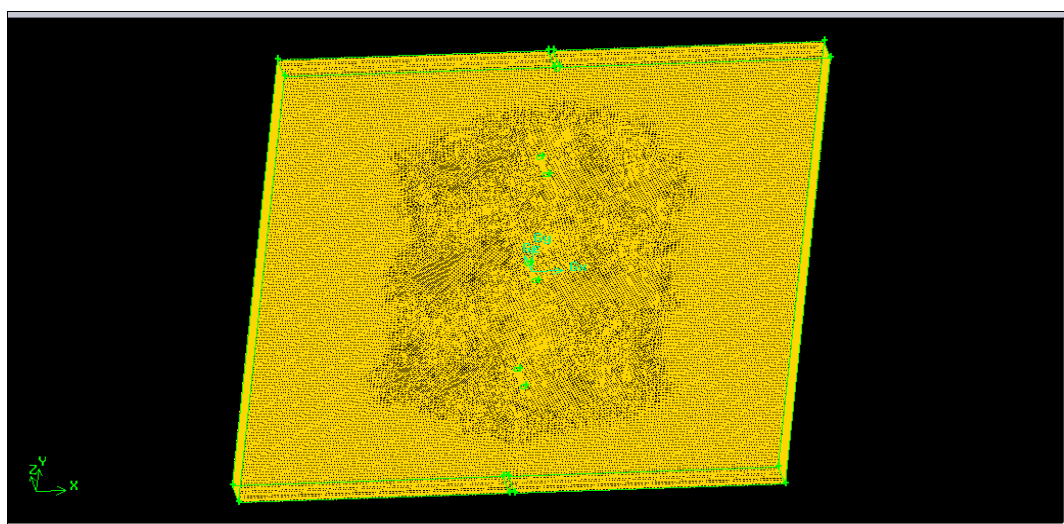


Fig.4 Mesh File by using GAMBIT

Boundary Condition

The diameter of cylindrical pier is 241m for numerical simulation and the material used for the bed are sand with specific weights of 2600 kg/m^3 , mean particle sizes of 0.0001m . The inlet boundary is placed at 241m from the center of the pier. At the inlet boundaries, the type of boundary was set as velocity-inlet. In simulation, water velocity is 1.09 ms^{-1} , 0.85 ms^{-1} and the inlet boundary is placed at 241m from the center of the pier. The type of boundary conditions is set as outflow. At the top surface, wall boundary conditions are used. The wall boundary is set at the bottom of sand. Pier is set as a slip wall boundary.

Two phases (water and sand) were set up. The top layer is set up water phase and bottom layer sand phase respectively. The two phase (water and sand) Eulerian model is used in order to simulate the local scour. For the Eulerian model, FLUENT provides Laminar and $k-\epsilon$ turbulence model. Here, $k-\epsilon$ turbulence model is employed to simulate.

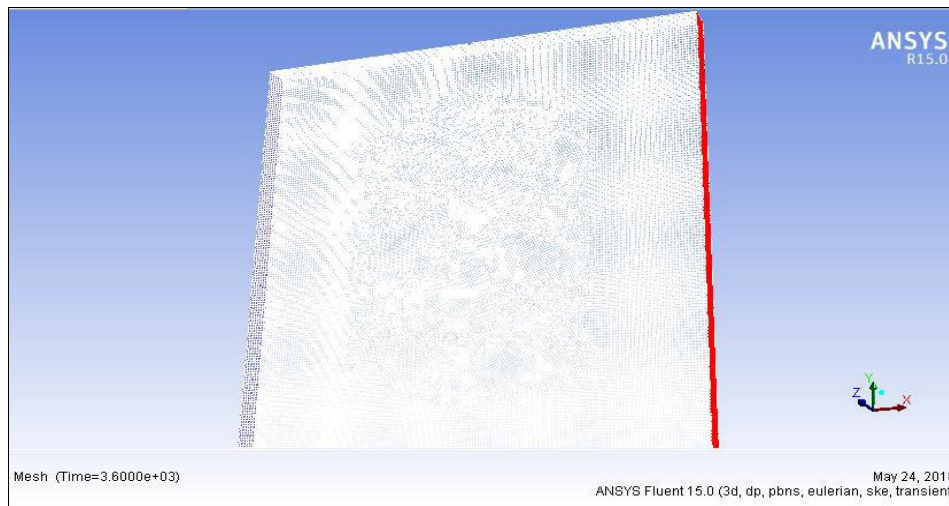


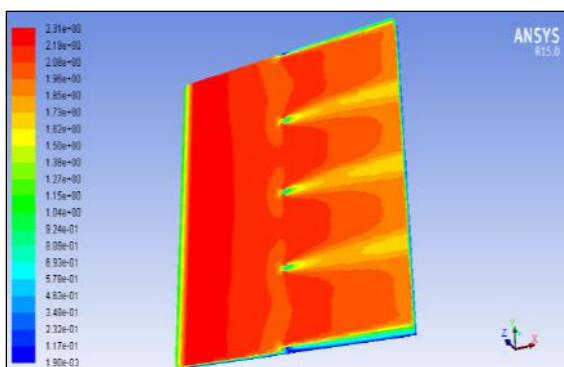
Fig.5 Using FLUENT to calculate pier scour

6. RESULTS:

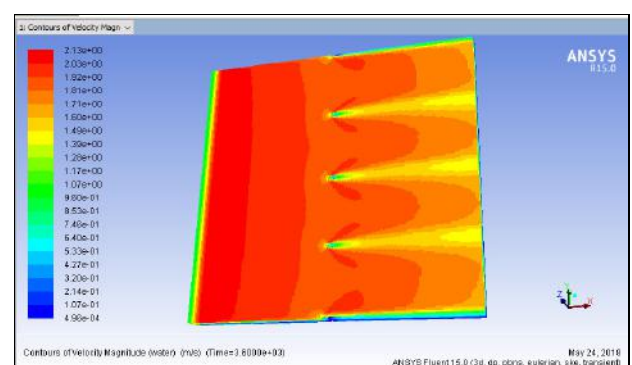
Numerical Simulation Results

The numerical modelling procedure of the multiphase flow is made up of two steps. The first step is geometry preparing and mesh generating. In the second step the flow field is calculated, after defining the general and multiphase model, phases and their interactions, viscous and turbulence model, boundary conditions, accuracy of numerical discretization, and initialization of the flow field. After obtaining solution convergence, post-processing and analysis of results are made.

The numerical solution predicts velocities in the x, y and z directions. The velocity contour and the velocity vector around the cylindrical structure is analysed using ANSY Fluent. In this study, simulation time step is 1(seconds) and number of time steps is 3600. Maximum iteration per time step is 5. The variation of different flow parameters are presented in the Fig. 6.



(b) 2016

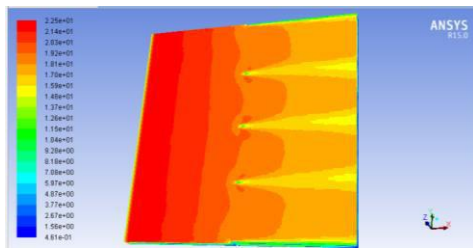


(a) 2017

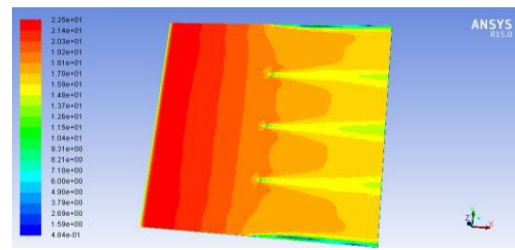
Fig.6(a,b) Contours of velocity magnitude by FLUENT

Scour depth around piers in 2017

Fig. 7(a, b) represents the scour depth contours at the piers. Two different mean diameter of particle size values considered in this simulation work are 0.0001, and 0.0002 m. It has been observed through these figures that increasing particle size values have considerably changed the scour depth especially in the regions of pier.



(b) mean diameter particle size = 0.0001



(a) mean diameter particle size = 0.0002

Fig.7(a,b) Contours of scour depth by FLUENT

Comparison of scour depth around bridge pier between numerical simulation and field observation in 2017

In 3-D simulation, change of velocity magnitudes and development of scour around pier were found reasonably. The comparison of scour depth between numerical simulation and observation are described in Fig. 8 and 9. The computed maximum scour depth for 2016 is 22.4m at P-7 for Maubin Bridge. The bed level for that is 21.7m. The result bed level is 21.65m that can be compared with the depth 18.9m at P-6. The computed maximum scour depth is 12m that can be compared with the depth 0.2m.

Similarly, next simulation is done for 2017. The computed maximum scour depth is 21.65m at P-7 for Maubin Bridge. The bed level for that is 21.3m. The result bed level is 21.65m that can be compared with the depth 20.1m at P-6. The computed maximum scour depth is 11.9m that can be compared with the depth 0.1m.

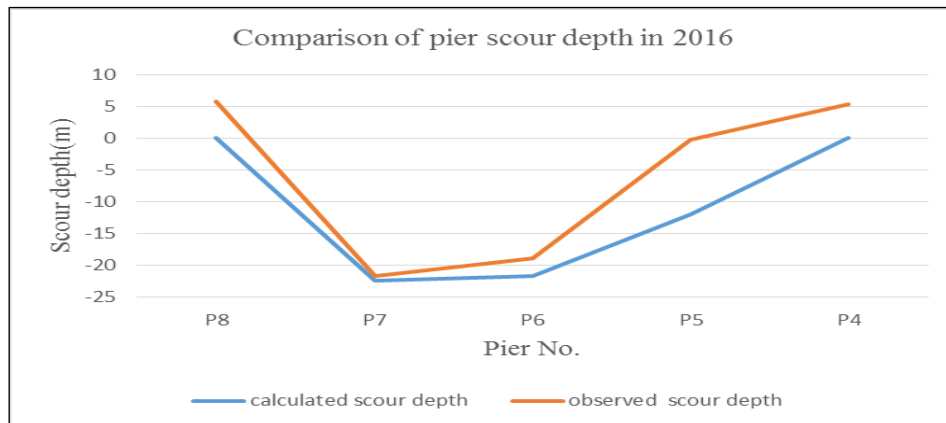


Fig.8 Comparison of scour depth around bridge pier in 2016

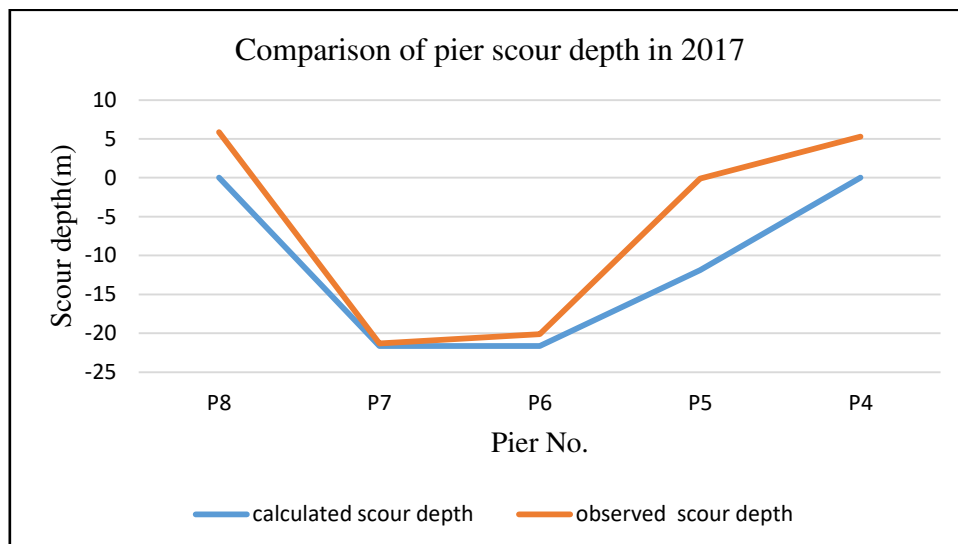


Fig.9 Comparison of scour depth around bridge pier in 2017

7. DISCUSSION AND CONCLUSION:

The numerical prediction scheme provided by CFD and experiment are used to predict the flow patterns of local scour around pier. The research has an important application in formulating numerical model of complex piers that include river bathymetry and bridge geometry so that scour can be predicted. Local scour is a direct consequence of the flow obstruction caused by the bridge. It is a time dependent process. The basic mechanism causing local scour at piers is the formation of horseshoe vortex.

During the Numerical solution, it was observed that the scour depths deeper and deeper at the midpoint of the upstream face of cylindrical pier. Simulated results show reasonable agreements with observation results. The comparisons between observation results and numerical results show that the mathematical model can simulate the process of local scour around pier and can obtain equilibrium profiles which are similar to observation results.

REFERENCES:

1. L.A. Arneson, L.W. Zevenbergen, P.F. Lagasse, P.E. Clopper, "Evaluating Scour at Bridges. Fifth Edition" U.S. Department of Transportation, Federal Highway Administration.
2. Sabita Madhvi Singh & P. R. Maiti, "Flow Field and Scouring around Cylindrical Structure in Channel Bed", Proc. of the Second Intl. Conf. on Advances In Civil, Structural and Environmental Engineering- ACSEE 2014.
3. Padmini Khwairakpam, Dr. Asis Mazumdar (May 2009). "Local Scour Around Hydraulic Structures", International Journal of Recent Trends in Engineering, Vol. 1, No. 6,.
4. Z. Zhang and B. Shi (2016), "Numerical Simulation of Local Scour around Underwater Pipeline based on FLUENT Software", Journal of Applied Fluid Mechanics, Vol. 9, No. 2, pp. 711-718,.
5. QIPING YANG (2005), "Numerical Investigations of Scale Effects on Local Scour around a Bridge Pier", The Florida State University, FAMU-FSU College of engineering ,October 28,
6. HAYDER MAJEED , NIGEL WRIGHT & ANDREW SLEIGH,(2015) "Large eddy simulations and analyses for bridge scour development" E-proceedings of the 36th IAHR World Congress, The Hague, the Netherlands, 28 June – 3 July,
7. B. D. ADHIKARY, P. MAJUMDAR, and M. KOSTIC, "CFD Simulation of Open Channel Flooding Flows and Scouring Around Bridge Structures", Proceedings of the 6th WSEAS International Conference on FLUID MECHANICS (FLUIDS'09)
8. Nazila KARDAN, Yousef HASSANZADEH, Habib HAKIMZADEH,(2012) "Comparison of Dynamic Bed Shear Stress Distribution around a Bridge Pier Using Various Turbulence Models", ICSE6-283, August 27-31,
9. ANSYS, Inc. Southpointe 275 Technology Drive, Canonsburg, PA 15317 "ANSYS Fluent Theory Guide", November 2013.
10. Vernon R. Bonner, Gary W. Brunner,(April 1996), "Bridge Hydraulic Analysis with HEC-RAS", US Army Corps of Engineers, Institute for Water Resources, Hydrologic Engineering Center,.